Sustainable Energy, Grids and Networks 44 (2025) 101888

Contents lists available at ScienceDirect

Sustainable Energy, Grids and Networks

journal homepage: www.elsevier.com/locate/segan

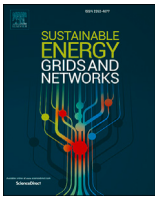

A methodology for the analysis and selection of weather station location for dynamic line rating using the estimation of effective wind

R. Minguez [a], R. Martinez [b,*], M. Manana [b], A. Arroyo [b], E. Sainz-Ortiz [c]

[a] Viesgo Distribución Eléctrica Grupo EDP, C/Isabel Torres 25, Santander, 39011, Cantabria, Spain
[b] GTEA, Departamento de Ingeniería Eléctrica y Energética, Universidad de Cantabria , Av. Los Castros s/n, Santander, 39005, Cantabria, Spain
[c] GTEA, Departamento de Transportes y Teznología de Proyectos y Procesos, Universidad de Cantabria , Av. Los Castros s/n, Santander, 39005, Cantabria, Spain

ARTICLE INFO

PACS:
84.70.+p
88.80.H
88.80.hh
88.50.Mp
88.05.Bc
88.80.Cd

Keywords:
Dynamic line rating
Digital elevation model
Weather station location
Wind propagation
Renewable integration

ABSTRACT

The new outlook regarding energy and climate change encourages electricity companies to increase the renewable power capacity and improve the infrastructure to manage and transport renewable energy. The increase in renewable energy, especially wind generation, together with the growth of distributed generation, creates the need to provide the flexibility to operate a grid. The economic, environmental and administrative barriers to creating new infrastructure or modifying existing infrastructure encourage the development of alternatives such as Dynamic Line Rating (DLR) systems. This study solves one of the problems that appear in the practical application of DLR systems. The aim of this study is to create a new methodology that allows the analysis of the error caused by an existing configuration of a DLR system and to determine the most appropriate number and location of measurement points during the design phase. These approaches are based on the Simulated Wind Distributed Estimation (SWDE) methodology, which obtains a cooling model along the line using wind propagation software and Digital Elevation Models.

1. Introduction

The new outlook regarding energy and climate change involves numerous actors, including electricity companies. Generation, transport and distribution are tasks that have a significant impact on action against climate change and renewable energy is the most important. The European Union proposes to achieve at least a 32 % share of renewable energy by 2030, but this target has been reached in Spain with a renewable energy production of 45.5 % of the total energy generated, with wind generation contributing to a 22.5 % of the production, in 2020 [1]. These challenges not only increase the installed renewable power capacity but also improve the infrastructure to manage and transport renewable energy. The increase in renewable energy, especially wind generation, together with the growth of the distributed generation [2,3], creates the need to provide flexibility to operate a grid. Economic, environmental and administrative barriers to creating new infrastructure or modifying existing infrastructure encourage the development of alternatives. Nowadays, solutions such as Dynamic Line Rating (DLR) provide the flexibility to operate the grid with non-invasive techniques, low investments and successful outcomes. The DLR is a smart grid technology that calculates the maximum current that an overhead line can transport without damaging the conductor.

Viesgo, a Spanish electricity company of the EDP Group, deployed Dynelec, a model for the use of DLR, on its overall 132 kV overhead grid [4]. This operational model is extremely favourable in grids where wind energy has a large share in the generation mix. In the case of Viesgo, the implementation of this system has allowed the overrating of critical lines, under favourable conditions, up to 214 % of their nominal rate, decreasing wind curtailments by 99 % [5].

Despite the significant development of DLR techniques, a few problems exist in the practical application of this technique. The deviations between the estimations and measurements in the conductor temperature were obtained during the operational phase. The main reasons for these deviations were errors in sensors used for estimations [6], errors in the procedures of estimation [7] and errors due to spot measurements

* Corresponding author.
Email address: raquel.martinez@unican.es (R. Martinez).

https://doi.org/10.1016/j.segan.2025.101888
Received 24 January 2025; Received in revised form 14 April 2025; Accepted 28 July 2025
Available online 25 August 2025

instead of distributed measurements [8]. Based on this, it is evident that the number and location of the measurement points along the lines are crucial to obtaining satisfactory results in DLR integration [9,10]. There are multiple options for operating a DLR system [11]. The most technically suitable option is to install a Distributed Temperature Sensor (DTS) and multiple weather stations distributed along the line to monitor its conditions. However, this option presents the disadvantage of high cost. Some existing DLR options search for the best location for the weather stations (WS), the least cooled spots of the line, to estimate the most restrictive ampacity along the line. These critical points are usually obtained through microclimatic studies along the line. These microclimatic studies are not trivial, and their classic result is qualitative but not quantitative. In [10], a heuristic was presented for developing a monitoring strategy, including the definition of the number and location of monitoring stations. This model is based on the use of weather model data, specifically the Weather Research and Forecasting (WRF) mesoscale atmospheric model. The WRF database consists of simulations at 1-km horizontal resolution and 10-m vertical resolution. However, this is a mesoscale model, and in the case of the wind, the effects of the terrain on the wind flow are so significant that a microscale model is needed. In [12], the authors propose a methodology to identify critical spans for DLR systems that warrant no infringement of ground clearance in any span and minimize sagging. In this case, a weather study was conducted using historical data for 10 years from 25 weather stations along the study line. Therefore, a large amount of weather data is needed to conduct the study.

The aim of this study is to create a new methodology that allows the analysis of the error produced by an existing configuration of a DLR system and to find the most appropriate number and location of the measurement points during the design phase. These methods are based on the SWDE methodology developed in [13]. The SWDE methodology, as outlined in [13], provides a cooling model for the line based on the effective wind. An important aspect of this paper is the sensitivity analysis of the DLR calculation procedure with respect to meteorological variables. The study concludes that wind is the variable with the greatest impact on the DLR calculation. This finding motivates the use of the methodology presented in this paper to analyse the errors produced by an existing configuration of a DLR system or to determine the most appropriate configuration during the design phase. The methodology relies on wind propagation software that uses the Digital Elevation Model of the location [14,15] and the height of the lines to estimate wind at the microscale along the line. This approach accounts for the significant role of wind in the DLR calculation procedure and addresses the challenges of obtaining microscale wind data. In this methodology, a simulation of the wind on a microscale based on the terrain and height of the conductor, provides an advantage over [10], since it provides a heuristic procedure based on the use of historical-simulated weather data, from a Mesoscale Weather Model. In addition, the methodology of this paper does not require WSs to be installed along the line to obtain historical data because the wind data are simulated by software, providing an advantage over the method in [12]. The most accurate system with which to compare the results would be the monitoring of the variables in a distributed manner along the line. However, as previously mentioned, the high cost of such a system makes its implementation highly complex. Although validation with real measured data is not available, the WindNinja software provides a very robust solution for microscale wind estimation. The proposed methodology is presented in Section 2, and the characteristics of the study lines are presented in Section 3. The results of the application of the proposed methodology are presented in Section 4. Finally, the summary of the study findings and its applications are presented in Section 5.

2. Methodology

In this section, a methodology with two complementary analyses is presented in Fig. 1. One of the analyses is to study the differences between the existing configuration of a DLR system and the minimum cooling along the line. The other analysis selects the optimum locations of the WSs to manage a line with the DLR system. The first analysis is appropriate for quantifying the error of an existing DLR system, whereas the second option is suitable for selecting the optimum number and locations of WSs in the design phase of a DLR system.

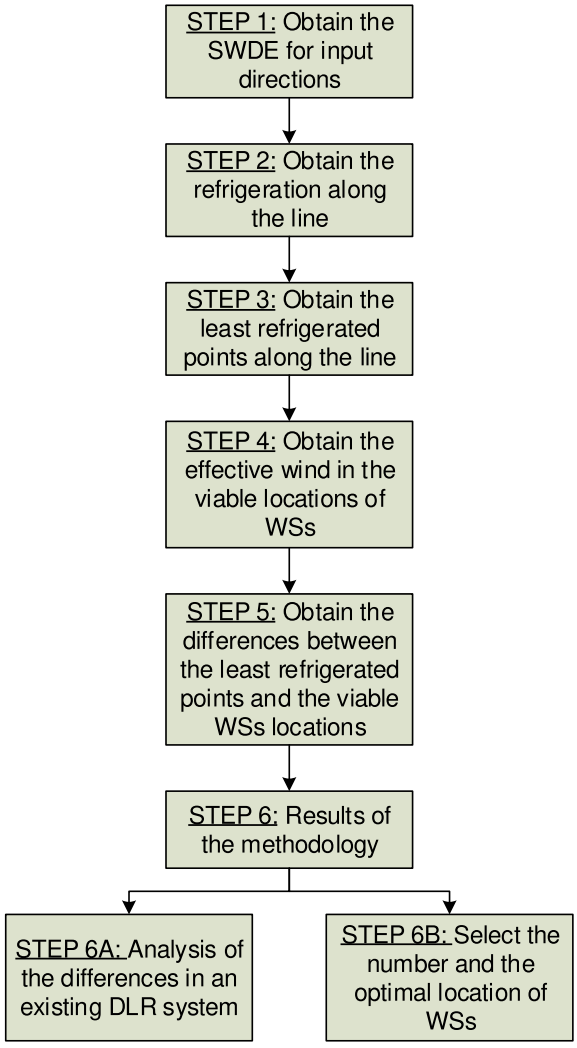

Fig. 1. Methodology flowchart.

DLR calculation is based on thermal balance equation defined by procedures [16] and [17].

$$q_s + q_J = q_c + q_r \tag{1}$$

where q_s is the heating due to solar radiation, q_J is the heating due to Joule effect, q_c is the cooling due to convection and q_r is the cooling due to radiation.

In general terms, and considering the most relevant variables, the thermal balance equation (1) accounts for, on the one hand, heating due to the Joule effect, ambient temperature, and solar radiation, and on the other hand, cooling by convection and radiation. Based on this, variables such as line current, ambient temperature, solar radiation, and wind are considered for the calculation. Other environmental variables, such as humidity or rainfall, may have some implications for the thermal balance of the conductor, but the calculation procedures analysed in this article do not take them into account. The impact of rainfall on ampacity calculation has been analysed in [18]. This study concludes that rainfall significantly enhances the thermal capacity of overhead lines due to its

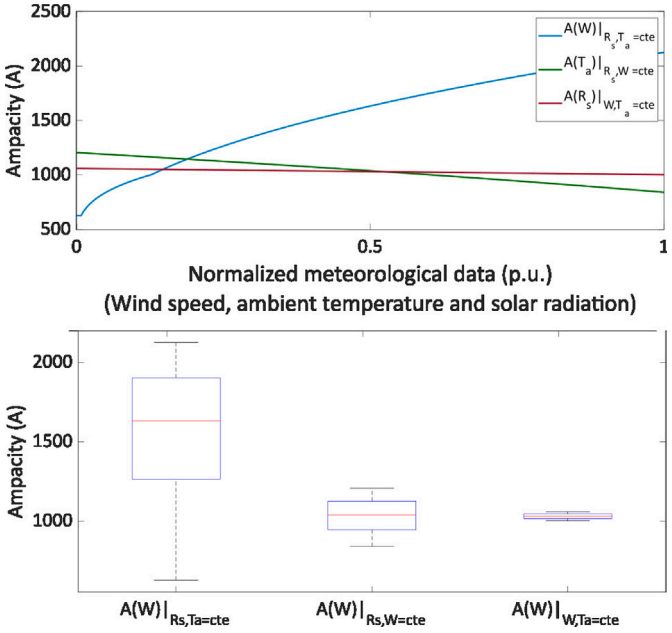

Fig. 2. Variation of ampacity with meteorological changes [13].

cooling effect. However, in the present methodology, the influence of rain will not be considered since the focus of this methodology is on identifying the least-cooled sections of the line as these are the most critical in determining the thermal limits of the conductor. Therefore, the presence of rain invariably results in conductor cooling, thereby improving ampacity values.

The methodology described in this paper is based solely on wind influence because of its significance in the ampacity calculation, as analysed in a previous study [13].

In this analysis, the significance of each meteorological variable (wind, ambient temperature, and solar radiation) was determined based on the ampacity variability with changes in meteorological variables and the variability of meteorological variables. The conclusions achieved in this analysis based on Fig. 2 are that the variability of the ampacity with the wind (on average around 1500 A/p. u) is much higher than that with ambient temperature (on average, approximately −200 A/p. u) or solar radiation (on average, approximately −50 A/p. u). In addition, in the analysis of the variability of the weather conditions, the coefficient of variation of solar radiation is the largest (1.610), followed by that of wind speed (1.422), and finally that of ambient temperature (1.388). Although the variability of the solar radiation was higher than that of the others, the variation in the ampacity with solar radiation was practically zero. In conclusion, the sensitivity analysis justified the approach of this study, which focused only on wind to select the critical point.

2.1. Step 1: obtain the simulated distributed wind estimation (SWDE) for input directions

The aim of the methodology is to use the level of cooling along the line to determine the most appropriate locations for installing WSs or to verify whether the locations of the WSs in an existing DLR system are appropriate. As discussed earlier, the level of cooling is obtained based on the wind alone owing to its significance in the ampacity calculation. The ideal case to obtain the level of cooling would be to install multiple WSs along the line to measure the wind every few meters because the wind at low altitudes varies significantly owing to the effects of the terrain. However, this solution is neither technically nor economically feasible. The most suitable solution was presented in a previous paper [13]. In

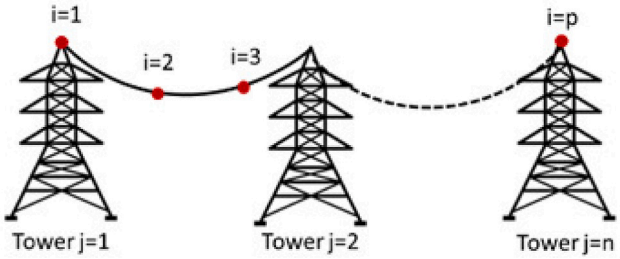

Fig. 3. Overhead line sample.

this study, the wind along the line was simulated using the WindNinja software and a digital elevation model of the location.

The aim of this step is to obtain the simulated wind distribution estimation (SWDE) along the line following the methodology described in [13].

For a given overhead line composed of n towers and n-1 spans (Fig. 3), the cooling model of the line is calculated using the SWDE methodology. The inputs required to calculate the SWDE are as follows:

- The Digital Elevation Model (DEM) along the line obtained using LiDAR technology.
- The height of the conductor along the line.
- Initial input wind speed at a given height.
- Initial input wind direction.

The DEM and wire heights were obtained using LiDAR technology. These data, together with the input wind (Eq. 2), were used as the inputs for the WindNinja software [14,15]. The input wind is a vector represented by the input wind speed w_{in}^{k} in m/s and the input wind direction φ_{in}^{k} in degrees. The input wind is defined as the wind at the mesoscale level at high heights, without considering the terrain, obstacles, or lines. In the first stage of the study developed in [13], the input wind provided to WindNinja software was a speed between the maximum and minimum wind in the area with a 1° variation in the direction. Based on the results obtained in this stage, the conclusion was that the wind speed results were linear. Thus, for the purpose of comparing the levels of cooling along the line, only the wind direction had an impact. Accordingly, it was possible to fix the input wind speed at 1 m/s and then obtain the rest of the input wind speeds in a linear manner. Therefore, the length of the input wind vector depends on the number of defined input wind angles (q). Typically, the input wind angles are defined to cover all possible wind directions (0°–360°) with the desired resolution. This ensures that the study achieves the level of cooling along the line for all possible winds, allowing the critical points to be located.

$$\begin{bmatrix} \left(w_{in}^{1} \middle| \varphi_{in}^{1}\right) \\ \left(w_{in}^{2} \middle| \varphi_{in}^{2}\right) \\ \cdot \\ \cdot \\ \cdot \\ \left(w_{in}^{q} \middle| \varphi_{in}^{q}\right) \end{bmatrix} \tag{2}$$

A wind propagation matrix (Eq. 3) is obtained using the WindNinja software with the input data. The software down-scaled the wind, at the height of the line, after taking into account the DEM information. This represents the wind propagation of the overhead line at the selected sampled points and is formed by the wind speeds (w_i^k) and wind directions (α_i^k), where i is the n-th sample point ($1 \le i \le p$) and k is the n-th input wind direction ($1 \le k \le p$). This matrix has as many columns as sample

points along the line and as many rows as the wind input angles.

$$\begin{bmatrix} \left(w_1^1 \middle| \alpha_1^1\right) & \left(w_2^1 \middle| \alpha_2^1\right) & . & . & . & \left(w_p^1 \middle| \alpha_p^1\right) \\ \left(w_1^2 \middle| \alpha_1^2\right) & \left(w_2^2 \middle| \alpha_2^2\right) & . & . & . & \left(w_p^2 \middle| \alpha_p^2\right) \\ . & . & . & . & . & . \\ . & . & . & . & . & . \\ . & . & . & . & . & . \\ \left(w_1^q \middle| \alpha_1^q\right) & \left(w_2^q \middle| \alpha_2^q\right) & . & . & . & \left(w_p^q \middle| \alpha_p^q\right) \end{bmatrix} \tag{3}$$

2.2. Step 2: obtain the cooling along the line

In [13], the effective wind was defined to represent the cooling of the line with one parameter, which encompasses the wind speed and attack angle of the wind. The effective wind is the equivalent perpendicular wind to the conductor, with the same cooling effect as the calculated wind. The calculation of the effective wind is based on the Morgan equations [19]. The wind propagation matrix is transformed into an effective wind matrix as shown in Eq. (4). This matrix (we_i^k) represents the cooling in all the i sample points along the line for each k input wind direction. This matrix has as many columns as the sample points and as many rows as the wind input angles.

$$\begin{bmatrix} we_1^1 & we_2^1 & . & . & . & we_p^1 \\ we_1^2 & we_2^2 & . & . & . & we_p^2 \\ . & . & . & . & . & . \\ . & . & . & . & . & . \\ . & . & . & . & . & . \\ we_1^q & we_2^q & . & . & . & we_p^q \end{bmatrix} \tag{4}$$

2.3. Step 3: obtain the least cooled points along the line

Once the cooling along the line is obtained, the least refrigerated vector along the line ($we\_\min^k$) is derived from the minimum value of the effective wind for each input wind direction k (Eqs. 5 and 6). This vector has as many rows as the wind input angles and represents the minimum cooling value of the line for each input angle.

$$we_{min}^k = min_{\forall i \in [1,p]} \left(we_i^k\right) \tag{5}$$

$$\begin{bmatrix} we_{min}^1 \\ we_{min}^2 \\ . \\ . \\ . \\ we_{min}^q \end{bmatrix} \tag{6}$$

The vector of least cooled points (l^k) is a vector with points along the line with the minimum effective wind for each input wind direction k (Eq. 7). The vector of the least refrigerated locations represents the sampled points of the line with less cooling and has as many rows as wind input angles (Eq. 8).

$$l^k = i \in [1,p] \text{ where } we_i^k = we_{min}^k \tag{7}$$

$$\begin{bmatrix} l^1 \\ l^2 \\ . \\ . \\ . \\ l^q \end{bmatrix} \tag{8}$$

2.4. Step 4: obtain the effective wind in the viable locations of WSs

Operationally, a WS is located on a tower, and consequently, i and p will be replaced by j and n, respectively, where j is the n-th tower along the line and n is the total number of towers (Fig. 3).

The effective wind matrix at the towers (wet_j^k) represented in Eq. (9) is extracted from the effective wind matrix in Eq. (4). This matrix represents the effective wind at the location of the towers for each input wind angle k. This matrix has as many columns as there are towers and as many rows as there are input wind angles.

$$\begin{bmatrix} wet_1^1 & wet_2^1 & . & . & . & wet_n^1 \\ wet_1^2 & wet_2^2 & . & . & . & wet_n^2 \\ . & . & . & . & . & . \\ . & . & . & . & . & . \\ . & . & . & . & . & . \\ wet_1^q & wet_2^q & . & . & . & wet_n^q \end{bmatrix} \tag{9}$$

2.5. Step 5: obtain the differences between the least cooled points and WS locations

The aim of this step is to calculate the differences between the minimum effective wind along the line and the effective wind at the towers. These differences allow us to identify the best locations for the WSs and measure the error for each combination of WSs.

There are several possibilities for locating WSs depending on the number of WSs (m) and the number of towers (n). For this reason, the number of possible combinations of WSs' locations (NC) is defined to assess the scenarios.

$$NC = C_n^m = \frac{n!}{m!(n-m)!} \tag{10}$$

The effective wind of each combination of WSs (wet_g^k) is calculated as the minimum of the effective wind of the WSs included in this combination where g is the index of each combination (Eq. 11). For this purpose, a list of NC tuples $L = (T_1, T_2, \ldots, T_g, \ldots, T_{NC})$ of m elements is defined. Each tuple $T_g = (T_{g,1}, T_{g,2}, \ldots, T_{g,u}, \ldots, T_{g,m})$ contains the indices of the towers where the WSs are located for each combination g. The wet_g^k matrix has as many columns as the number of combinations and as many wind angles. For each tuple of combinations and wind angle,

$$wet_g^k = min_{\forall u \in [1,m]} \left(wet_{T_{g,u}}^k\right) = \min\left(wet_{g,1}^k, wet_{g,2}^k, \ldots, wet_{g,m}^k\right) \tag{11}$$

The differences between the minimum effective wind along the line and the effective wind at all locations of the WSs are depicted by the Root Mean Square Difference (RMSD). Therefore, the RMSD for each combination of WS locations was obtained using Eq. (12). Vector $RMSD_c$ has as many columns as the number of combinations (NC).

$$RMSD_g = \sqrt{\frac{\sum_{k=1}^{q} \left(we_{min}^k - wet_g^k\right)^2}{q}} \tag{12}$$

2.6. Step 6: results of the methodology

2.6.1. Step 6A: analysis of an existing DLR system

In existing DLR systems, it is important to analyse whether the locations of the WSs produce admissible difference values. In this step, the RMSD values of the actual locations of the WSs and those of the remaining options along the line are presented to assess if the difference level is admissible. The analysed values are the $RMSD_g$ for all values of g, which is equal to the location of the existing WSs.

2.6.2. Step 6B: select the number and the optimal location of WSs

During the design phase of a DLR system, it is important to assess the optimal number and location of WSs.

- Decide the number of WSs m. The number of WSs depends on several factors, including economic, orographic, and operational factors.
- The optimal locations of the WSs are selected. The WS combination with the lowest RMSD is chosen for placing the WSs.

The most commonly used operational factor is to fix an acceptable maximum RMSD and obtain the number and location of WSs that fulfil this requirement.

Additionally, the mean (Eq. 13), minimum (Eq. 14) and standard deviation of the selected WSs RMSD (Eq. 15) are calculated as follows:

$$RMSD_{mean} = \frac{\sum_{g=1}^{NC} RMSD_g}{NC} \tag{13}$$

$$RMSD_{min} = min_{\forall g \in [1,NC]} \left(RMSD_g\right) \tag{14}$$

$$SD = \sqrt{\frac{\sum_{g=1}^{NC} \left(RMSD_g - RMSD_{mean}\right)}{NC - 1}} \tag{15}$$

3. Materials and methods

The methodology explained in the previous section is applied to two overhead lines of 132 kV with different cooling characteristics. Line I is 90 km long and passes through mountainous areas (Fig. 4) and line II is 3 km long and is located in a gorge (Fig. 5).

The input variables used to apply the methodology developed in this paper are as follows:

- The Digital Elevation Model (DEM) of each line: 5 × 5 m cell size.
- The height of the conductor along the line for each line.
- Input wind speed: $w_{in} = 1$ m/s due to the linearity of the results.
- Input wind direction: $\varphi_{in} = [0 - 359]^{\circ}$ with a resolution of 1°.
- Sampled points: 1 pt/10 m ($p_{LineI} = 276$ and $p_{LineII} = 2914$). It is not meaningful to define more points than the resolution of the Digital Elevation Model (DEM), which corresponds to 1 pt/5 m. A compromise solution has been adopted between computational cost, since doubling the number of points results in a quadratic increase in computational demand, and accuracy, as variations in wind over distances shorter than 10 m have been observed to be negligible.
- Towers: $n_{LineI} = 16$ and $n_{LineII} = 647$.

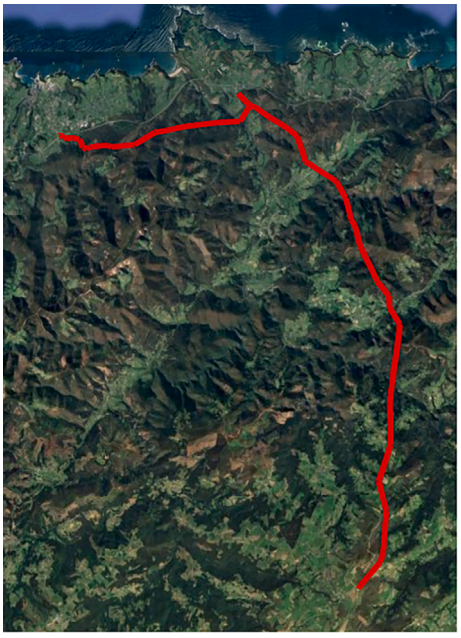

Fig. 4. Line I location.

Fig. 5. Line II location.

4. Results

The methodology described in this paper is applied to the study lines using the input data presented in Section 3. Due to the large amount of data generated throughout the various steps of the methodology, the process is summarised from Step 6 onwards by calculating the $RMSD_{min}$ for the optimal reference case with the WSs in each tower ($n_{LineI} = 647$ and $n_{LineII} = 16$).

The values obtained in this study are based on the wind differences between the different points of the line and least cooling points. These values are easy to assess to determine whether the point is appropriate for locating a WS. To understand the results of this study, it is important to compare the wind difference results of the methodology with the accuracy of the possible weather stations installed on the line. Because of the large number of weather stations on the market and the differences in accuracy between them, the accuracy of the WSs, specifically the accuracy of the wind measurements, will be based on the guidelines published by the World Meteorological Organization [20]. According to this guide, the accuracy requirements for wind measurements are as follows:

- Wind Speed
  - Range: 0–75 m/s
  - Measurement uncertainty: 0.5 m/s for <5 m/s and 10 % for >5 m/s
- Wind Direction
  - Range: 0°–360°
  - Measurement uncertainty: 5°

On the basis of the above, RMSD values below 0.5 m/s, when wind speed is below 5 m/s, and 10 % of wind speeds, when wind speed is above 5 m/s, would not be conclusive. In this study, owing to the linearity of the input wind, an input wind speed of only 1 m/s was required for the calculations. For this reason, the uncertainty would be 0.5 m/s.

4.1. Step 6A: analysis of an existing DLR system

In order to analyse the performance of an existing location of WS, three use cases, for one, two, and three WSs located in all possible combinations along the line are assessed. This assessment involves calculating the difference between each combination and the lowest cooling point. Figs. 6 and 7 show three histograms with the RMSD values of each combination, allowing a comparison of the actual configuration with the rest of the options. The DSO can analyse this comparison to determine whether the error level is assumable or contrary, and it is necessary to change the location of the WSs to improve the difference.

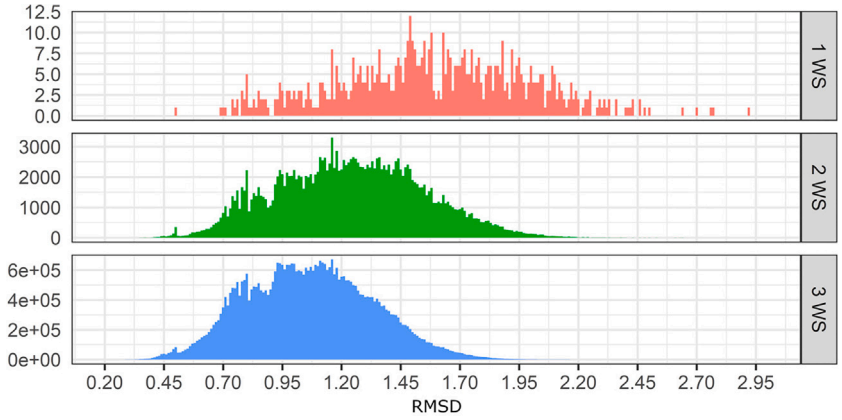

Fig. 6. RMSD values for different combinations of Line I.

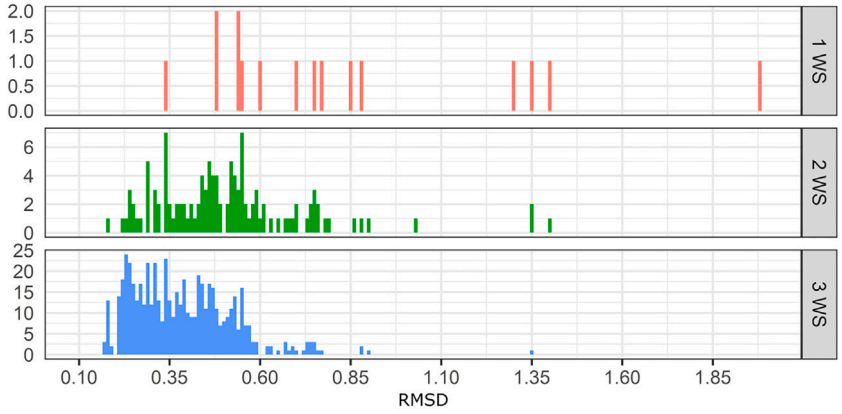

Fig. 7. RMSD values for different combinations of Line II.

In Figs. 6 and 7, the histograms of the results of the different cases of WS locations are shown. It can be seen that, for Line I, the selection of the WS locations could imply maximum and minimum errors of 2.90 m/s and 0.43 m/s, respectively, for 1 WS; approximately 2.20 m/s and 0.325 m/s, respectively, for 2 WSs; and approximately 1.95 m/s and 0.325 m/s, respectively, for 3 WSs.

Regarding Line II, the maximum and minimum errors are 1.975 m/s and 0.35 m/s respectively for 1 WS, 1.413 m/s and 0.225 m/s respectively for 2 WSs and 1.35 m/s and 0.2 m/s respectively for 3 WSs.

These figures are simple to analyse to determine if the existing DLR configuration is appropriate or if it is possible to make improvements regarding the location or number of WSs.

4.2. Step 6B: select the number and the optimal location of WSs

- Decide the number of WSs (m):

  The methodology explained previously is applied to eight different cases regarding the number and location of WSs. These eight cases were selected to analyse the best approach considering several criteria:

  – Reference case with one WS on each tower obtaining the minimum error. The study needs a reference case to compare with the rest. The ideal reference case would be the installation of infinite WSs along the line to know the weather conditions in all the points of the line. In view of the technical impossibility of this, the most realistic possible case would be the installation of one WS on each tower. For that reason, the reference case of this study is considered the highest resolution monitoring system. This is a non-realistic case for a real implementation due to technical and economic reasons, but it is used as a reference case to obtain the deviation of every case with respect to the optimal one.
    - ⁎ Case VI: WSs located in all the towers of the line (m = n).
  – Setting the number of WS.
    - ⁎ Case I: one WS placed in the best location (m = 1).
    - ⁎ Case II: two WSs placed in the two best locations (m = 2).
    - ⁎ Case III: three WSs placed in the three best locations (m = 3).
  – Setting the acceptable maximum RMSD.
    - ⁎ Case IV: the necessary WSs to reach the 80th percentile of $RMSD_g$.
    - ⁎ Case V: the necessary WSs to reach the 95th percentile of $RMSD_g$.
  – Most common settings in real DLR systems.
    - ⁎ Case VII: two WSs are located in substation feeders (m = 2).
    - ⁎ Case VIII: three WSs, two located in substation feeders and one in the optimal location (m = 3).This optimal location is the tower that provides $RMSD_{min}$ in combination with the WSs of the substation feeders.

  The procedure to obtain $RMSD_g$ for Cases IV and V is different because otherwise, the number of combinations would be too high. Therefore, it is not feasible to calculate it for all combinations of WSs; instead, an iterative procedure has been used. It consists of choosing the best location of the first WS. Similarly, for Case 1, one WS is calculated and remains selected, and the second WS is chosen using the same procedure, which is performed iteratively until the desired $RMSD_g$ is obtained. Although the methodology includes a combinatorial analysis to evaluate all possible WS configurations,

Table 1
Results for Line I.

Case number	Location (l)	NC	RMSD (m/s)			
			Max	Mean	Min	SD
Case I	507	647	2.919	1.588	0.498	0.400
Case II	507,646	208,981	2.641	1.237	0.346	0.308
Case III	473, 507,646	44.930.915	2.579	1.066	0,253	0.265
Case IV	507,646,473,647,337, 326,410,474,557,504	6,425	0.096	0.096	0.096	–
Case V	507,646,473,647,337, 326,410,474,557,504, 631,421,22,607,198	9,600	0.08	0.08	0.08	–
Case VI	1 to 647	1	0.074			–
Case VII	1,647	1	0.637			–
Case VIII	1,473,647	645	0.637	0.553	0.359	0.067

Table 2
Results for Line II.

Case number	Location (l)	NC	RMSD (m/s)			
			Max	Mean	Min	SD
Case I	4	16	1.983	0.844		0.444
Case II	4,1	120	1.404	0.512	0.185	0.213
Case III	4,1,9	560	1,347	0.384	0,166	0.139
Case IV	4,1	31	0.185	0.185	0.185	–
Case V	4,10,1,2	58	0.161	0.161	0.161	–
Case VI	1 to 16	1	0.147	–		
Case VII	1,16	1	0.474	–		
Case VIII	1,9,16	14	0.474	0.344	0.229	0.092

the results demonstrate that a sequential selection approach—adding WSs iteratively based on minimum RMSD—yields practically identical results in terms of critical station identification. The differences between the sequential and full combination approaches are negligible. Therefore, the computational burden is significantly reduced without loss of accuracy. This confirms that heuristic methods, applied after obtaining the complete effective wind profiles for all wind directions, can be a valid and efficient alternative to brute-force evaluation. The proposed methodology inherently incorporates this concept, offering a low-cost yet reliable solution for optimal WS placement.

- Select the optimal locations of the WSs. The m points of the $RMSD_g$ with the lowest values are selected to place the WSs. The results are presented in Tables 1 and 2.

Table 1 represents the results for the Line I. As can be observed, depending on the case under study, both the number and the location of critical points vary. The cases range from requiring a single weather station in Case I to needing up to 12 weather stations in Case V. For this line, the most critical points are located in spans 507, 646 and 473. It is worth highlighting that, in most common real DLR system cases, Case VII and VIII, the average of the differences can reach values of 0.637 and 0.553 m/s, respectively, representing an increase of approximately 700 % with respect to the reference case, Case VI.

Table 2 represents the results for de Line II. In the case of this line the cases range from requiring a single WS in Case I to needing up to 4 WSs in Case V. For this line, the most critical points are located in spans 4, 1 and 9. It is worth highlighting that, in most common real DLR systems cases, Case VII and VIII, the average of the differences can reach values of 0.474 representing an increase of approximately 200 % with respect to the reference case, Case VI.

Therefore, it should be emphasised that, for both lines, operating under the configurations of Case VII and VIII could lead to ampacity values significantly exceeding the most restrictive limit of the lines, which may result in damage to the electrical lines.

Fig. 8. 3D Image of the least cooled towers for Line I.

As a complementary analysis, 3D images of the location of the lines for Cases I, II, and III are shown to verify whether the location of the least cooled towers is associated with terrain characteristics (Figs. 8 and 9).

As shown in Fig. 8, towers 473 and 507 are clearly located at points with an orography that prevents cooling. In the case of Tower 546, although it is in a more open location, winds from the north are blocked by the mountain.

In Fig. 9, towers 1 and 4 are clearly located at points with an orography that prevents cooling. In the case of tower 9, the reason for the lack of cooling is less clear.

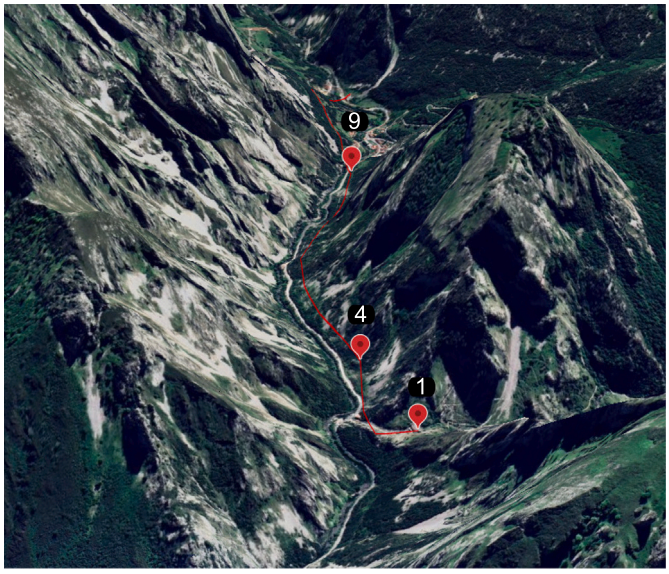

Fig. 9. 3D Image of the least cooled towers for Line II.

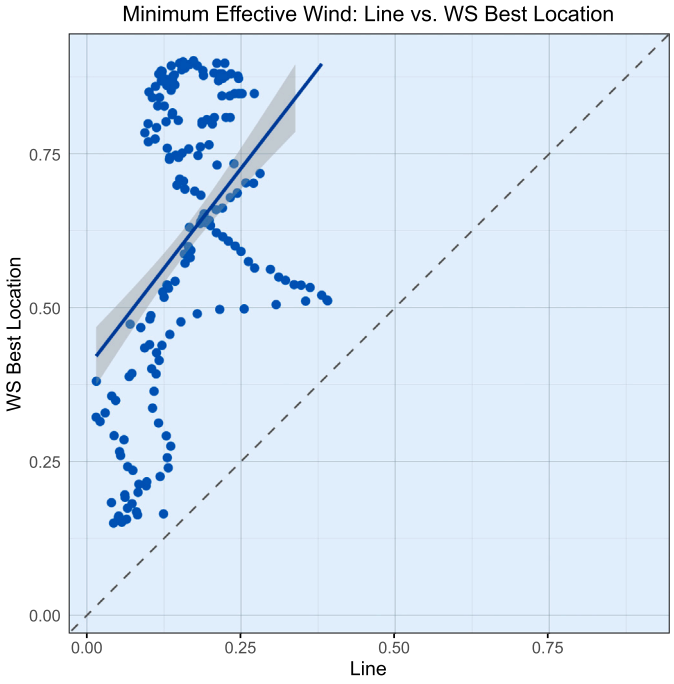

Fig. 10. Correlation between minimum effective wind along the line vs. effective wind in the location of the WS for Case I and Line I.

Valuable insight into the effectiveness of the proposed methodology is provided by Figs. 10 and 11. These figures illustrate the correlation between the minimum effective wind along the line and the wind at the optimal position of the WSs. In this case, the results correspond to Case I, in which only one WS is selected. For Line I, a certain degree of correlation can be observed in some cases, particularly in the points that lie close to the blue line. However, these points deviate significantly from the actual minimum effective wind along the line, represented by the dashed line. In contrast, for Line II, although no clear correlation is apparent in the vicinity of the blue line, there are multiple points that coincide with the minimum effective wind along the line—points that align with the dashed line.

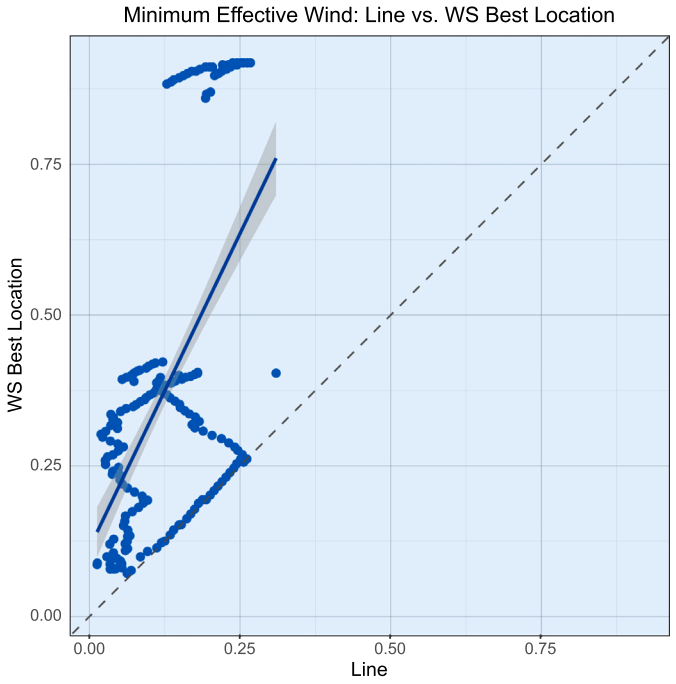

Fig. 11. Correlation between minimum effective wind along the line vs. effective wind in the location of the WS for Case I and Line II.

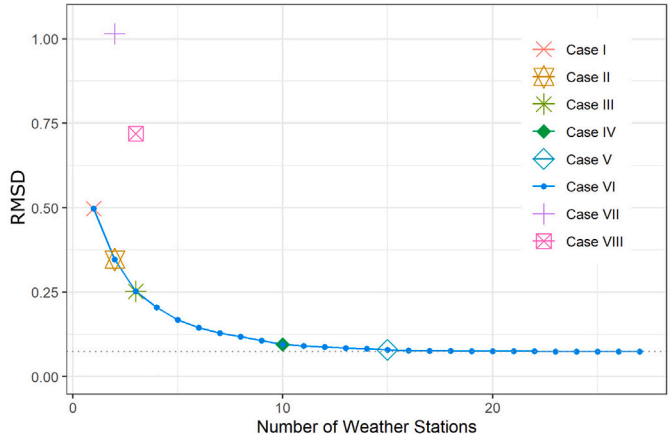

Fig. 12. Evolution of RMSD with number of WSs in Line I.

The comparison among the eight cases allows us to observe the evolution of RMSD and assess the most appropriate system.

Figs. 12 and 13 show the evolution of RMSD with the number of WSs. In the case of Line I, only the first 27 WSs are represented because the RMSD does not improve when more WSs are added. In the case of Line II, all possible numbers of WSs are represented.

Figs. 14 and 15 represent the evolution of the difference between each case and the minimum effective wind of the line, respectively. This is an interesting way to represent the importance of the number and location of WSs and the influence of wind direction. In these figures, they represent the minimum effective wind of the line (we^k_{min}) and the minimum effective wind for each case (we^k_g) for all cases and for all wind directions.

For Line I, in Case I, the level of error is high and highly dependent on the wind direction. Adding one weather station (Case II), the error is reduced by 30 % and remains highly dependent on the wind direction. With another WS (Case III), a 50 % reduction in the error

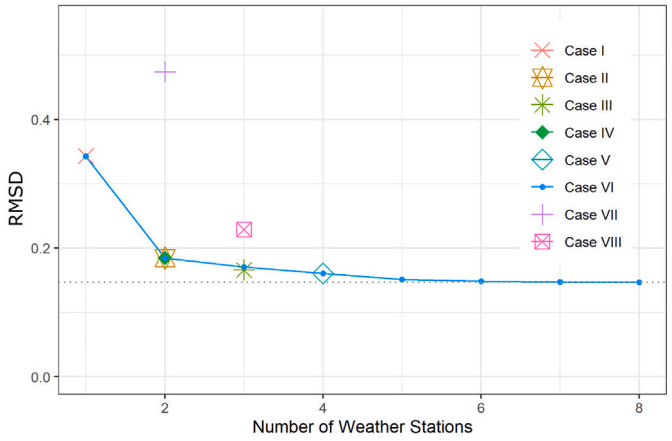

Fig. 13. Evolution of RMSD with number of WSs in Line II.

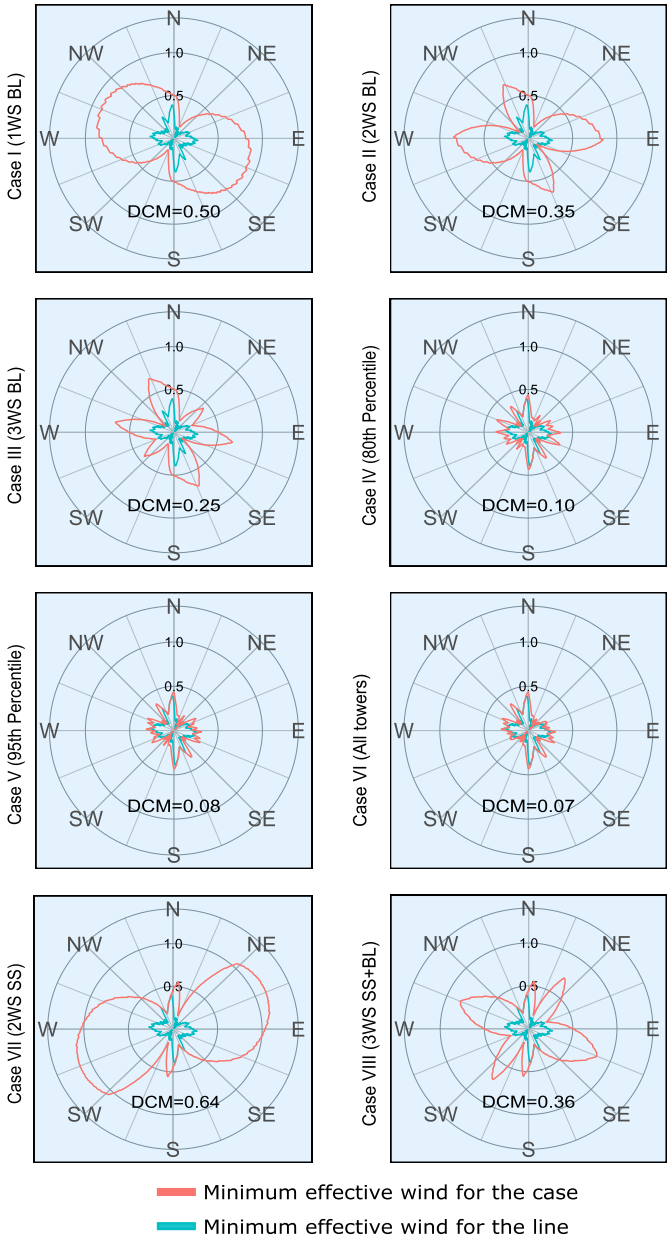

Fig. 14. Evolution of the difference between each case and the minimum effective wind of the line for Line I.

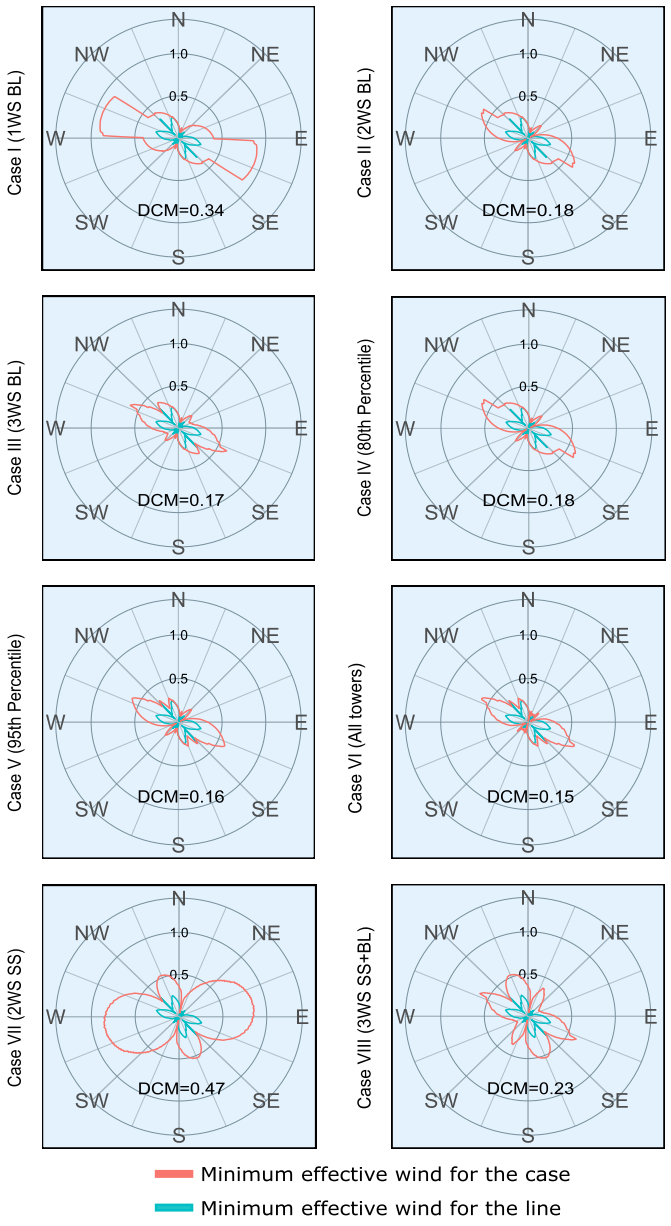

Fig. 15. Evolution of the difference between each case and the minimum effective wind of the line for Line II.

is achieved in case I, and this system is less dependent on the wind direction. For cases IV, V, and VI, the errors are reduced by approximately 85 % and are practically independent of the wind direction. These cases required 10, 15, and 647 weather stations, respectively. Finally, the cases most commonly used in DLR systems, Cases VII and VIII, obtained very different results with high levels of differences. In this line, based on Fig. 12, it is possible to improve the differences by adding more WSs until the differences stabilise at approximately 16 WSs, at which point increasing the number of stations no longer improves the differences.

For Line II, in Case I, the level of difference is lower than that in Line I and is highly dependent on the wind direction. Adding one weather station (Case II), the difference is reduced by 50 % and remains highly dependent on the wind direction. With another WS (Case III), a significant difference is not achieved from case II. The same occurred for cases IV, V, and VI. These cases required 2, 4, and 16 weather stations, respectively.

Finally, the cases used more in DLR systems, Cases VII and VIII, obtained very different results with high levels of differences.In this line, based on Fig. 13, they could achieve the minimum value of difference with 6 WSs, and at this point increasing the number of stations no longer improves the differences.

5. Discussion

For line I and one WS, the error moved from 0.498 m/s to 2.912 m/s, with a mean error value of 1.588 m/s and a standard deviation of 0.400 m/s. For the same line with three WSs, the difference between the best and worst combinations was 0.253 m/s and 2.579 m/s, the mean error was 1.066 m/s, and the standard deviation was 0.265 m/s. As expected, with a larger number of WSs, the error distribution histogram is narrower and the mean value is smaller (Figs. 6 and 7).

As shown in Figs. 12 and 13,in the case of Line I, Cases VII and VIII have higher errors than Cases I, II, and III although they have more or the same number of WSs. In the case of Line II, Cases VII and VIII have higher errors than Cases II and III, although they have the same number of WSs. Therefore, differences between the effective wind at a position and the minimum effective wind are more dependent on the location than the number of WSs.

In the cases discussed in this paper, the best way to monitor the line with the lowest number of WSs is to install approximately ten WSs in Line I and four in Line II. The biggest drawbacks of these systems are the large investment required and the communication and supply problems associated with installing WSs in remote places.

The evolution of the error in both Line I and Line II decreases when fitting a power trendline, with a higher rate of decline in Line I.

It is important to note that although this practical approach is characteristic of these two lines, results demonstrate that the location and number of WSs in a DLR are key points for deploying a high-performance DLR system.

6. Conclusions

This article presents a methodology that allows both the study of whether an existing configuration of a DLR system has an appropriate error margin and the definition of the most suitable configuration for a DLR system in the design phase. Two study lines with very different cooling characteristics have been used, which allow conclusions to be drawn that can be generalised to other lines.

Several conclusions regarding the number, location, and combinations of WSs were obtained in this study. This methodology allows the quantification of both the number and location of WSs for the maximum allowable error set by the distribution company. This maximum error will be established in such a way as to prevent line assets ageing. The error for the specific configuration of a set of weather stations was quantified.

Firstly, it can be concluded that the differences between the effective wind at a position and the minimum effective wind are more dependent on the location than the number of WSs. This conclusion is crucial, as the goal when defining WSs configuration in a DLR system is not to have a large number of WSs, but rather to strategically locate them at key points, even if this means having fewer WSs.

Another important conclusion is that, considering the lines studied, the most commonly used cases in practice (Cases VII and VIII) do not represent the best results from the point of view of differences between the effective and minimum effective winds in a position. In addition, in cases with a low number of WSs, the differences are highly dependent on the angle of the wind.

The general conclusion of the article is that this methodology could improve existing approaches for determining the most suitable WSs configuration for a DLR system included in the state of the art (microclimatic studies, heuristic procedures, etc.) offering greater accuracy than the solutions more commonly adopted by distribution companies (Case VII and Case VIII). Furthermore, it enables the estimation of errors in existing systems, allowing for an assessment of whether these errors are acceptable—something that was not possible to evaluate until now.

It is important to understand that the application of this methodology for defining the DLR system configuration during the design phase will be based on the DEM available at the planning stage. Electricity companies typically perform LIDAR flights every few years, which provide a periodic update of the line's DEM. Therefore, if significant changes in the DEM are observed, the methodology can be reapplied to assess the errors introduced in an existing system using the updated DEM and to evaluate whether these remain within the acceptable limits defined by the company. If the results fall outside those limits, a new analysis can be carried out to determine the most appropriate locations for the WSs.

On the other hand, it is important to highlight the limitations of this methodology. The most notable limitation is the lack of validation in a real-world environment. As previously mentioned, validation through distributed wind measurements along the line is virtually unfeasible due to the economic implications associated with such a deployment. In this case, however, this limitation is mitigated by the robustness of the results obtained with WindNinja, a well-established and widely used software for microscale wind simulation. In future work, a system will be implemented to partially verify the methodology using real measurements on the lines, employing new low-cost and easy-to-install sensors.

CRediT authorship contribution statement

R. Minguez: Writing – review & editing, Validation, Methodology, Formal analysis, Writing – original draft, Software, Investigation, Data curation, Visualization, Project administration, Funding acquisition, Conceptualization. **R. Martinez:** Visualization, Methodology, Writing – review & editing, Validation, Investigation, Writing – original draft, Resources, Formal analysis. **M. Manana:** Project administration, Formal analysis, Writing – review & editing, Investigation, Validation, Funding acquisition. **A. Arroyo:** Project administration, Formal analysis, Writing – review & editing, Investigation, Validation, Funding acquisition. **E. Sainz-Ortiz:** Writing – review & editing, Formal analysis, Validation, Investigation.

Declaration of competing interest

The authors declare that they have no known competing financial interests or personal relationships that could have appeared to influence the work reported in this paper.

Acknowledgments

This publication is part of the R&D&I project PID2023-151457OB-I00, funded by MICIU/AEI/10.13039/501100011033/ and, as appropriate, by "ERDF A way of making Europe", by "ERDF/EU", by the "European Union" or by the "European Union NextGenerationEU/PRTR". Furthermore, this publication was funded by University of Cantabria Industrial Doctorate 19.DI12.649 (BOC 206, 26th October 2016). The authors express their gratitude to Viesgo Distribution and EDP for permitting the use of company information that was relevant to this article.

Data availability

The data that has been used is confidential.

References

[1] Red Eléctrica de España (REE), The Spanish Electrical System 2020, 2021, https://www.ree.es/sites/default/files/publication/2021/03/downloadable/avanceISE2020EN.pdf.

[2] R. Cossent, T. Gómez, P. Frías, Towards a future with large penetration of distributed generation: is the current regulation of electricity distribution ready? Regulatory recommendations under a European perspective, Energy Policy 37 (3) (2009) 1145–1155, ISSN 0301-4215, https://doi.org/10.1016/j.enpol.2008.11.011.

[3] H. Zhang, Effects of distributed generation on grid system: a survey, Int. J. Grid Distrib. Comput. 9 (8),2016) 307–318, https://doi.org/10.14257/ijgdc.2016.9.8.27.
[4] M. Mañana, R. Martinez, A. Arroyo, P. Castro, R. Minguez, A. Gonzalez, R. Garrote, A. Laso, R. Domingo, Metodología para el cálculo y predicción de la ampacidad en líneas eéctricas aéreas, segúnla elección de los emplazamientos críticos, ES2569431B1.
[5] R. Minguez, R. Martinez, M. Manana, A. Arroyo, R. Domingo, A. Laso, Dynamic management in overhead lines: a successful case of reducing restrictions in renewable energy sources integration, Electr. Power Syst. Res. 173 (2019) 135–142, ISSN 0378-7796, https://doi.org/10.1016/j.epsr.2019.03.023.
[6] CIGRE, TB 299. Guide for selection of weather parameters for bare overhead conductor ratings, 2006.
[7] A. Arroyo, P. Castro, R. Martinez, M. Manana, A. Madrazo, R. Lecuna, A. Gonzalez, Comparison between IEEE and CIGRE thermal behaviour standards and measured temperature on a 132-kVoverhead power line, Energies 8–12 (Dec. 2015) 13660–13671. MDPI.
[8] R. Martinez, A. Useros, P. Castro, A. Arroyo, M. Manana, Distributed vs. spot temperature measurements in dynamic rating of overhead power lines, Electr. Power Syst. Res. 170 (2019) 273–276.
[9] G. Molinar, M. Li, W. Stork, Positioning of distributed weather overhead line monitoring based on historical weather data, in: 2019 IEEE AFRICON, 2019, pp. 1–6, https://doi.org/10.1109/AFRICON46755.2019.9134046.
[10] M. Matus, et al., Identification of critical spans for monitoring systems in dynamic thermal rating, IEEE Trans. Power Deliv. 27 (2) (Apr. 2012) 1002–1009, https://doi.org/10.1109/TPWRD.2012.2185254.
[11] D.A. Douglass, et al., A review of dynamic thermal line rating methods with forecasting, IEEE Trans. Power Deliv. 34 (6) (Dec. 2019) 2100–2109.
[12] J. Teh, I. Cotton, Critical span identification model for dynamic thermal rating system placement, IET Gener. Transm. Distrib. 9 (2015) 26442652.
[13] R. Minguez, R. Martinez, M. Manana, D. Cuasante, R. Garañeda, Application of digital elevation models to wind estimation for dynamic line rating, Int. J. Electr. Power Energy Syst. 134 (2022) 107338, ISSN 01420615, https://doi.org/10.1016/j.ijepes.2021.107338.
[14] J.M. Forthofer, B.W. Butler, N.S. Wagenbrenner, "A comparison of three approaches for simulating fine-scale surface winds in support of wildland fire management". Part I. Model formulation and comparison against measurements, Int. J. Wildland Fire 23 (2014) 969–981.
[15] N.S. Wagenbrenner, J.M. Forthofer, B.K. Lamb, K.S. Shannon, B.W. Butler, Downscaling surface wind predictions from numerical weather prediction models in complex terrain with WindNinja, Atmos. Chem. Phys. 16 (2016) 5229–5241, https://doi.org/10.5194/acp-16-5229-2016.
[16] CIGRE, TB 601. Guide for Thermal Rating Calculations of Overhead Lines, 2012.
[17] IEEE, IEEE std 738-2012. Standard for Calculating the Current-Temperature of Bare Overhead Conductors, 2012.
[18] A. Abdaelbaset, M.E. Farrag, S. Farokhi, Evaluation of precipitation rate impacts on overhead transmission line ampacity, in: 2019 54th International Universities Power Engineering Conference (UPEC), Bucharest, Romania, 2019, pp. 1–5, https://doi.org/10.1109/UPEC.2019.8893644.
[19] V.T. Morgan, Thermal Behaviour of Electrical Conductors, Steady, Dynamic and Fault-Current Ratings, Taunton, Somerset, England; New York, 1991. Research Studies Press; Wiley, Electronic & Electrical Engineering Research Studies, Lines and Cables for Power Transmission Series; vol. 5, xvii + 741 pp., 0863801196, 0471930717.
[20] Guide to Instruments and Methods of Observation, World Meteorological Organization (WMO), 2020.